TECHNICAL REPORT

nature neuroscience

In vivo auditory brain mapping in mice with Mn-enhanced MRI

Xin Yu[1,2], Youssef Zaim Wadghiri[1,3], Dan H Sanes[4] & Daniel H Turnbull[1,2,3,5]

There are currently no noninvasive imaging methods available for auditory brain mapping in mice, despite the increasing use of genetically engineered mice to study auditory brain development and hearing loss. We developed a manganese-enhanced MRI (MEMRI) method to map regions of accumulated sound-evoked activity in awake, normally behaving mice. To demonstrate its utility for high-resolution (100-μm) brain mapping, we used MEMRI to show the tonotopic organization of the mouse inferior colliculus. To test its efficacy in an experimental setting, we acquired data from mice experiencing unilateral conductive hearing loss at different ages. Larger and persistent changes in auditory brainstem activity resulted when hearing loss occurred before the onset of hearing, showing that early hearing loss biases the response toward the functional ear. Thus, MEMRI provides a sensitive and effective method for mapping the mouse auditory brainstem and has great potential for a range of functional neuroimaging studies in normal and mutant mice.

A fundamental goal of neurobiology research is to determine the genetic and molecular basis for the development of brain function. At present, knowledge of the genetic factors underlying normal and abnormal mammalian brain development has been obtained primarily from experiments performed in mice, often using transgenic and gene targeting approaches. In contrast, our understanding of brain physiological function is largely derived from experiments performed in larger rodents and primates in which genetic information and manipulation tools are unavailable. Although *in vivo* electrophysiological data can be obtained in mice, the acquisition of these data is difficult and is often a limiting factor in attempts to link genetic factors involved in brain development with the resulting effects on adult brain function. These facts underscore the clear and critical need to develop sensitive and effective large-scale, noninvasive methods for mapping physiological parameters in the mouse brain.

Neuroimaging methods such as functional magnetic resonance imaging (fMRI), based on blood oxygenation level–dependent (BOLD) magnetic resonance imaging (MRI) contrast[1], have revolutionized neuroscience research by providing noninvasive approaches to map neural activity in living animals and humans. However, fMRI in the mouse brain remains a challenging and largely unexplored area. Although there is an increasing availability of high-field MRI systems for anatomical microimaging in small animals, the implementation of robust BOLD-fMRI with sufficient spatial and temporal resolution for functional brain imaging in mice remains technically challenging. Even in humans, auditory brain mapping with fMRI is particularly difficult because of the challenges of decoupling the response to a defined auditory stimulus from the response to background noise produced by the MRI scanner.

An alternative MRI approach to image neural activity is provided by MEMRI, which makes use of the fact that paramagnetic manganese ions (Mn^{2+}) enter synaptically activated neurons through voltage-gated calcium channels[2], resulting in enhancement on T1-weighted MRI brain images. MEMRI detection of electrically and pharmaceutically induced activity has been demonstrated in the rat cortex[3] and validated by correlation with BOLD-fMRI[4]. Subsequently, MEMRI has been used to detect both hypothalamic activity and ischemia-induced excitotoxicity[5]. These studies in rats require surgical cannulation of the carotid artery during imaging for co-injection of manganese chloride ($MnCl_2$) with mannitol to transiently break the blood-brain barrier, and they are limited to detecting activity induced acutely during the narrow time window of mannitol-mediated blood-brain barrier permeability, primarily in anesthetized animals. At present, intra-carotid injection can be done only with difficulty in adult mice, precluding longitudinal studies at early developmental stages. In mice, the only previous report of functional imaging with MEMRI was the detection of odor-induced activity, using $MnCl_2$ aerosolized with specific odors to transport Mn^{2+} into the olfactory bulb[6]. Unfortunately, this approach is specific to the olfactory system and cannot be applied for mapping other brain regions.

We have developed a noninvasive MEMRI method for mapping accumulative sound-evoked activity in mice after systemic (intraperitoneal) administration of $MnCl_2$. Our results demonstrate a clear relationship between Mn^{2+} enhancement and sound-evoked activity and also show the feasibility of longitudinal imaging from early postnatal stages of mouse auditory brain development. To test the spatial accuracy of MEMRI brain mapping, we generated high-frequency tonotopic maps of the mouse inferior colliculus that were in excellent agreement with previously reported electrophysiological measurements. In mice, early unilateral hearing loss (before the onset of hearing) results in large and persistent changes in auditory

[1]Skirball Institute of Biomolecular Medicine, [2]Graduate Program in Neuroscience and Physiology and [3]Department of Radiology, New York University School of Medicine, 540 First Avenue, New York, NY 10016, USA. [4]Center for Neural Science, New York University, 4 Washington Place, New York, NY 10003, USA. [5]Department of Pathology, New York University School of Medicine, 540 First Avenue, New York, NY 10016, USA. Correspondence should be addressed to D.H.T. (turnbull@saturn.med.nyu.edu).

Published online 29 May 2005; doi:10.1038/nn1477

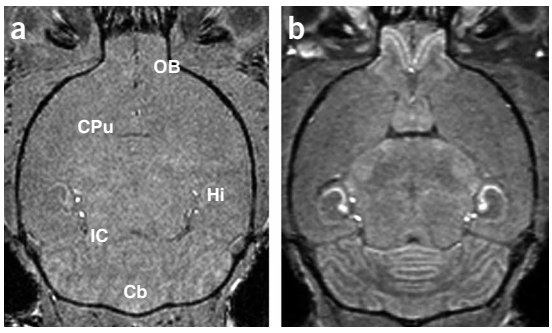

Figure 1 Mn-enhanced MRI (MEMRI) of the mouse brain under normal conditions. (**a**,**b**) Horizontal T1-weighted images of an adult mouse brain without Mn^{2+} (**a**) and 24 h after i.p. injection of $MnCl_2$ (**b**) demonstrated contrast enhancement in a number of brain regions: Cb, cerebellum; Hi, hippocampus; IC, inferior colliculus; OB, olfactory bulb. The caudate putamen (CPu) was identified as a region with no obvious MEMRI enhancement.

brainstem activity in the pathway ascending from the functional ear. MEMRI brain mapping can therefore be used to analyze auditory brain activity and plasticity in normal and surgically or genetically manipulated mice. It is likely that MEMRI can also be used to map other sensory systems in mice, providing an important new tool for analyzing gene-function relationships in the developing mammalian brain.

RESULTS

MEMRI provides region-specific brain enhancement

Systemic administration of $MnCl_2$ results in region-specific uptake of paramagnetic Mn^{2+} and subsequent enhancement on T1-weighted MR images under conditions of normal behavior[7–9]. We reasoned that using a defined stimulation approach, it should be possible to detect and analyze activity-related MEMRI enhancement after systemic administration of $MnCl_2$. In contrast to previous MEMRI reports in which activity was induced acutely and detected in anesthetized animals[3–5], we sought a method to detect accumulated activity resulting from repetitive stimulation of awake, normally behaving mice. Similar to previous studies[7,9], after intraperitoneal injection of $MnCl_2$ we observed maximum ventricular enhancement at 2 h post-injection, which cleared over the following 24 h; this was accompanied by a gradual increase in parenchymal enhancement that persisted for more than 48 h, with maximum enhancement around 24 h post-injection[9]. Furthermore, MEMRI signal intensities after injection of $MnCl_2$ were greatest in several specific brain regions, including olfactory bulb, hippocampus, midbrain and cerebellum (**Fig. 1**). Therefore, a challenge of employing MEMRI for functional neuroimaging is to decouple the activity-related enhancement attributable to a defined stimulation approach from nonspecific MEMRI enhancement. To explore the utility of MEMRI for mapping auditory brain activity in response to repetitive acoustic stimulation, we analyzed enhancement patterns 24 h after injection of $MnCl_2$, after the ventricular enhancement had cleared, when parenchymal enhancement was maximized.

MEMRI demonstrates sound-evoked activity

To examine the utility of MEMRI for detecting sound-evoked auditory activity in the mouse brain, we first compared signal intensities from images of normal mice and mice with bilateral conductive hearing loss (CHL), injected intraperitoneally with $MnCl_2$ and exposed to 24 h of broadband (1–59 kHz) frequency- and amplitude-modulated sound. This stimulus was designed to activate a wide range of auditory neurons that have different sensitivities to frequency, intensity or dynamic modulation of these parameters (**Supplementary Fig. 1**). We chose the CHL model because it specifically attenuates sound-evoked neural activity without deafferenting the central auditory pathway[10]. For each brain region under analysis, we defined a volumetric region of interest (ROI), comparing three-dimensional (3D) MRI data to a reference mouse brain atlas (**Fig. 2a**).

Comparisons of MEMRI signal intensities in normal and bilateral CHL mice showed statistically significant enhancement in the auditory

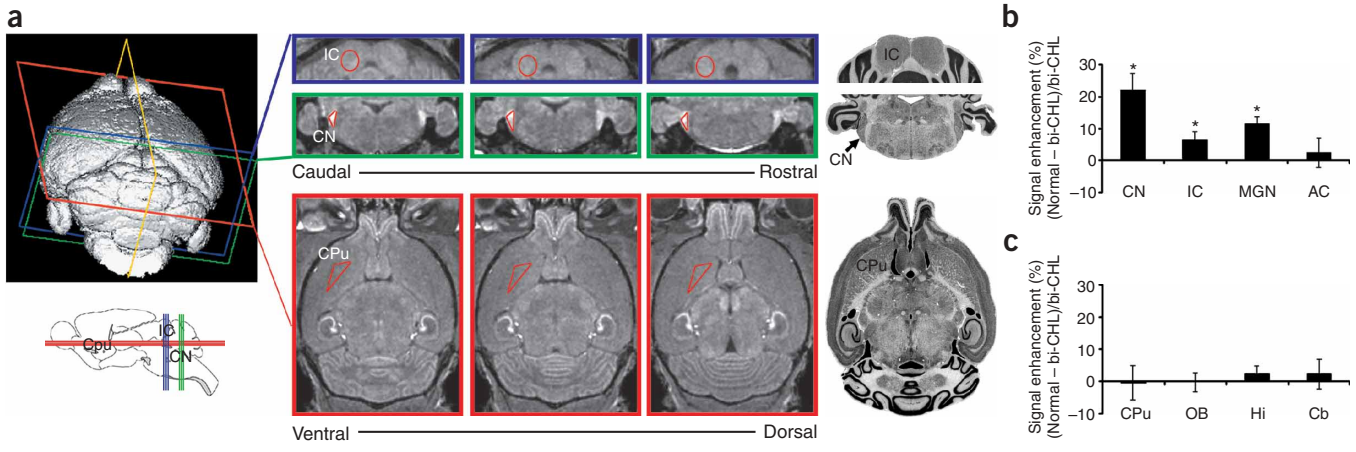

Figure 2 Brain regions were analyzed from volumetric *in vivo* MRI data. (**a**) Using 3D MRI data (upper left) with 100-μm isotropic resolution, auditory nuclei and control regions were identified in coronal or horizontal cross-sections (100 μm thick) through each region (central panels), and ROIs were defined (open red triangles or circles) after comparing MRI with a reference mouse brain atlas (right: reprinted with permission from the Mouse Brain Library, http://www.mbl.org). Three representative slices are shown through each of the auditory brainstem nuclei (green: CN, cochlear nucleus; blue: IC, inferior colliculus) and a non-auditory control region (red: CPu, caudate putamen). The orientations of sections through each nucleus are also indicated on the schematic sagittal representation of the mouse brain (lower left). (**b**,**c**) Quantitative comparison of MEMRI signal between normal mice ($n = 7$) and bilateral CHL mice ($n = 7$) in ascending auditory nuclei (CN; IC; MGN, medial geniculate nucleus; AC, auditory cortex; **b**) and in non-auditory brain regions, including regions with (Cb, cerebellum; Hi, hippocampus; OB, olfactory bulb) and without (CPu) obvious enhancement (**c**). Regions with statistically significant MEMRI enhancement are marked with an asterisk (*).

brainstem nuclei (cochlear nucleus, CN; inferior colliculus, IC) and thalamus (medial geniculate nucleus) ($P < 0.04$, $n = 7$, two-tailed *t*-test), whereas there was no significant enhancement in the primary auditory cortex (**Fig. 2b**). In non-auditory brain regions, there were no significant differences between normal mice and mice with bilateral CHL in both the caudate putamen (CPu) and in the regions most obviously enhanced under ambient conditions: olfactory bulb, hippocampus and cerebellum ($n = 7$; **Fig. 2c**). Furthermore, Mn^{2+} delivery and enhancement in each nucleus was highly consistent, as demonstrated by standard deviations of 2–5% in each brain region analyzed (**Fig. 2b,c**). Finally, enhancement was significantly higher in the CN and IC of mice exposed to broadband noise for 24 h than in mice maintained for the same period in a quiet environment ($P < 0.04$, $n = 7$, two-tailed *t*-test; **Supplementary Fig. 2**). These results strongly support the use of MEMRI enhancement as a relative measure of accumulated sound-evoked activity within auditory brainstem nuclei of mice.

Unilateral CHL: differential activity in individual mice

As MEMRI enhancement due to sound stimulation was significantly increased in auditory brainstem nuclei, we performed further experiments in mice with unilateral CHL, comparing MEMRI signal levels in the ascending pathways from either the functional or CHL ear, thereby providing an internal ipsilateral-contralateral comparison between auditory nuclei in each individual mouse. We produced equal numbers of mice with left ($n = 3$) and right ($n = 3$) unilateral CHL to avoid any possible bias in the measurements. We compared MEMRI signal levels between bilateral CHL mice ($n = 7$; **Fig. 3a**), unilateral CHL mice ($n = 6$; **Fig. 3b**) and normal mice ($n = 7$; **Fig. 3c**). In the CPu, a non-auditory structure, there were no differences in MEMRI signal level (**Fig. 3d**). To minimize potential differences due to variable delivery of Mn^{2+} after intraperitoneal injection, MEMRI measurements from CN and IC in each mouse were normalized to the corresponding CPu measurement.

We performed statistical analyses (two-tailed *t*-test) on MEMRI data from normal mice ($n = 7$), bilateral CHL mice ($n = 7$) and unilateral CHL mice ($n = 6$). Mice with unilateral CHL showed significant MEMRI enhancement in the ipsilateral CN compared with the contralateral CN, referenced to the functional ear ($P < 0.03$; **Fig. 3b,e**). Moreover, the signal differences between ipsilateral and contralateral CN in unilateral CHL mice were similar to the differences in CN signal between normal and bilateral CHL mice ($P < 0.0001$; **Fig. 3a,c,e**), although the ipsilateral CHL signal did not exceed that observed in normal mice. As expected from the known ascending axonal projections connecting CN to contralateral IC[11], mice with unilateral CHL showed significant MEMRI enhancement in the contralateral IC compared with the ipsilateral IC, referenced to the functional ear ($P < 0.0003$; **Fig. 3b,f**). As in the CN, the differences between ipsilateral and contralateral IC in unilateral CHL mice were similar to the differences in IC between normal and bilateral CHL mice ($P < 0.0003$; **Fig. 3a,e,f**). Histogram analysis further confirmed these differences, showing a higher distribution of CN signals in normal mice versus bilateral CHL mice ($n = 3$; **Fig. 3g**) and in ipsilateral CN versus contralateral CN in unilateral CHL mice ($n = 3$; **Fig. 3h**). A higher distribution of IC signals was also found in normal mice versus bilateral CHL mice ($n = 3$; **Fig. 3i**) and in contralateral IC versus ipsilateral IC in unilateral CHL mice ($n = 3$; **Fig. 3j**).

These results show that the unilateral CHL mouse provides a good model to compare activity levels in brainstem nuclei of individual mice, with and without direct auditory input. The *in vivo* MEMRI data presented here are in excellent agreement with *ex vivo* 2-deoxyglucose autoradiography results in the IC of gerbils with unilateral CHL[10], providing confirmation of these results with an independent methodology. Notably, the unilateral CHL mouse model can be used to examine the effects on brain function of hearing loss at different developmental stages, as described below.

MEMRI demonstrates the tonotopic organization of the IC

Frequency selectivity is a key feature of the central auditory system, originating in the encoding of frequencies along the length of the cochlea, and subsequently translated by means of specific afferent projections to each ascending nucleus. Electrophysiological methods have long been available for examining developmental changes in the tonotopic maps in the mouse brain[12,13] and continue to be used to characterize altered tonotopic representations associated with abnormal inner ear and auditory brain development[14]. An easily implemented, large-scale noninvasive MEMRI tonotopic mapping approach

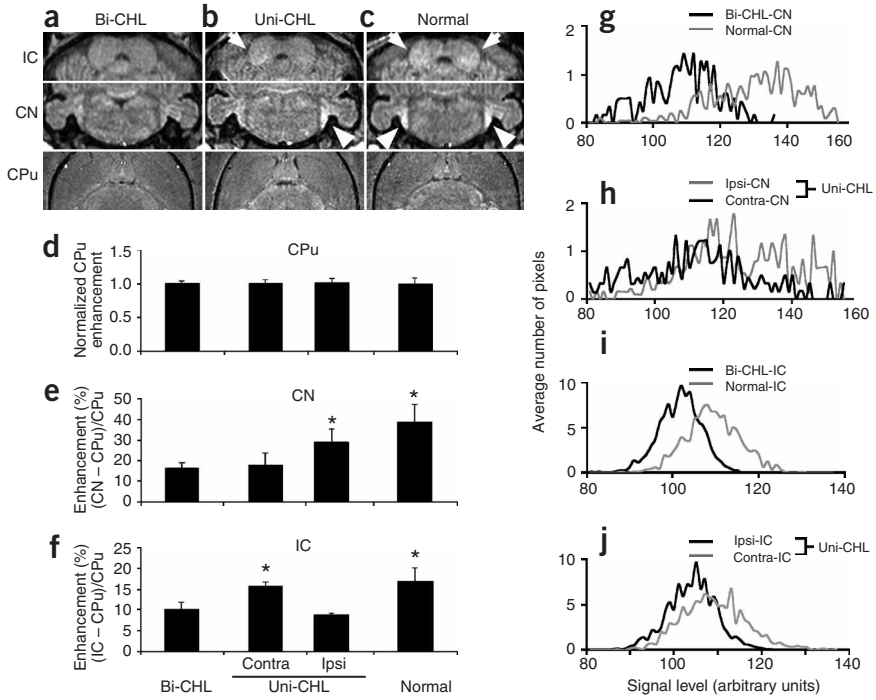

Figure 3 MEMRI enhancement in brainstem auditory nuclei was altered in mice with CHL. (**a**–**c**) Comparisons of individual mice with bilateral CHL (bi-CHL; **a**), mice with unilateral CHL (uni-CHL; **b**) and normal mice (**c**) demonstrated marked differences in MEMRI signals in the CN (arrow heads) and IC (arrows), but not in non-auditory CPu. (**d**–**f**) Quantitative analysis was performed on MEMRI signals from normal mice ($n = 7$), mice with bilateral CHL ($n = 7$) and mice with uni-CHL ($n = 6$). Statistically significant MEMRI enhancement is marked with an asterisk (*). (**g**–**j**) Averaged histograms ($n = 3$) of MEMRI signal levels comparing normal mice and bilateral CHL mice (**g**,**i**) and comparing ipsilateral signals to contralateral signals in the CN and IC of unilateral CHL mice (**h**,**j**).

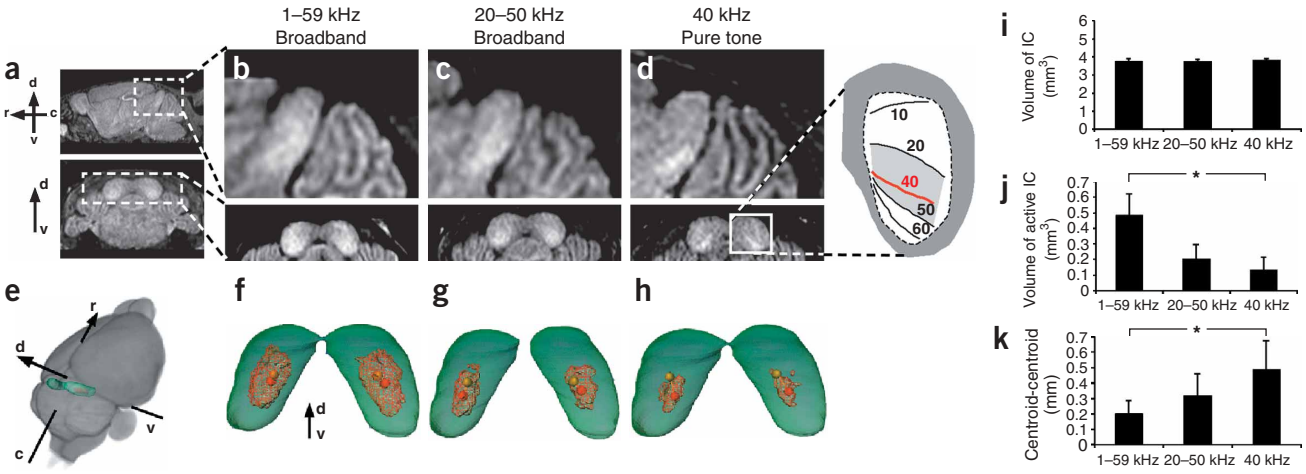

Figure 4 MEMRI was used to map the tonotopic organization of the mouse IC. (**a**) Sagittal (upper) and coronal (lower) images of the P21 IC showed obvious differences in mice exposed to defined stimuli. (**b**) After broadband (1–59 kHz) stimulation, enhancement covered most of the rostral-caudal (r-c), ventral-dorsal (v-d) extent of the central nucleus of the IC. (**c**) After high-frequency broadband (20–50 kHz) stimulation, enhancement was more restricted to the ventral-caudal region. (**d**) After 40 kHz pure-tone stimulation, enhancement was restricted to an isofrequency band in excellent agreement with electrophysiological maps[13] (inset). (**e**) Averaged, co-registered images ($n = 8$) were used to extract whole-brain (gray) and IC (green) and to generate 3D maps of MEMRI IC enhancement (red) after stimulation with 1–59 kHz (**f**), 20–50 kHz (**g**) and 40 kHz (**h**). From these 3D maps we determined the spatial coordinates of the centroids of both the IC (yellow spheres) and the enhanced volumes (red spheres). Measurements of IC volume (**i**), IC-enhanced volume (**j**), and position (distance between IC centroid and enhanced volume centroid; **k**) were made in the three experimental groups. Statistical analysis showed significant differences in both the enhanced volumes and the centroid-centroid distances between each pair of groups (*).

would complement existing electrophysiological methods, providing rapid assessment and new insights into altered tonotopic organizations in a variety of mouse models.

To assess the use of MEMRI for tonotopic mapping we focused on the high-frequency projection region of the central nucleus of the IC, as the mouse audiogram displays greatest sensitivity above 10 kHz (ref. 15). In addition, the low-frequency region of the tonotopic map includes the dorsomedial nucleus and dorsal cortex in the mouse, which are more prone to habituation to repetitive acoustic stimuli than the central nucleus[16].

In order to compare our results to previously published electrophysiological IC tonotopic maps[13], we performed MEMRI experiments on postnatal day 21 (P21) mice. We injected mice with $MnCl_2$ and exposed them, for 24 h before MRI, to sound stimulation with defined frequency characteristics (**Supplementary Fig. 1**): (i) broadband, 1–59 kHz; (ii) high-frequency broadband, 20–50 kHz and (iii) pure tone, 40 kHz. There were obvious differences in IC enhancement in the three experimental groups (**Fig. 4**): a diffuse pattern of enhancement covered most of the central nucleus after broadband stimulation (**Fig. 4b**,**f**), it was more confined to the ventral-caudal IC after high-frequency broadband stimulation (**Fig. 4c**,**g**), and it resolved into a clear ventral-caudal band after 40 kHz pure-tone stimulation (**Fig. 4d**,**h**). We made quantitative measurements of whole-IC volume ($n = 8$; **Fig. 4i**), enhanced-IC volume ($n = 8$; **Fig. 4j**) and enhanced-IC position ($n = 8$; **Fig. 4k**). Statistical analysis (one-way ANOVA) of these MEMRI data showed significant differences between the volumes ($F_{2,45} = 62.09$, $P < 0.0001$; **Fig. 4j**) and positions ($F_{2,45} = 16.71$, $P < 0.0001$; **Fig. 4k**) of the enhanced-IC regions in the three groups of mice. Furthermore, the dorsal-ventral depth of the 40 kHz isofrequency centroid, measured as a fraction of the full dorsal-ventral extent of the IC, was in excellent agreement with previously published electrophysiological maps[13] (MEMRI, 67 ± 4%, versus electrophysiology, 73 ± 6%). Auditory brain activity is known to have a complex dependence on both sound frequency and amplitude, and further experiments are required to determine the MEMRI representations of these complex activity patterns. These first results clearly demonstrate that MEMRI provides spatial sensitivity similar to *in vivo* electrophysiology and further verify MEMRI brain mapping.

We also performed tonotopic experiments to assess the utility of MEMRI for longitudinal brain mapping in individual mice. Specifically, each mouse was injected with $MnCl_2$ and exposed to high-frequency broadband (20–50 kHz) stimulation for 24 h before MRI to detect sound-evoked Mn^{2+} uptake in the IC, after which they

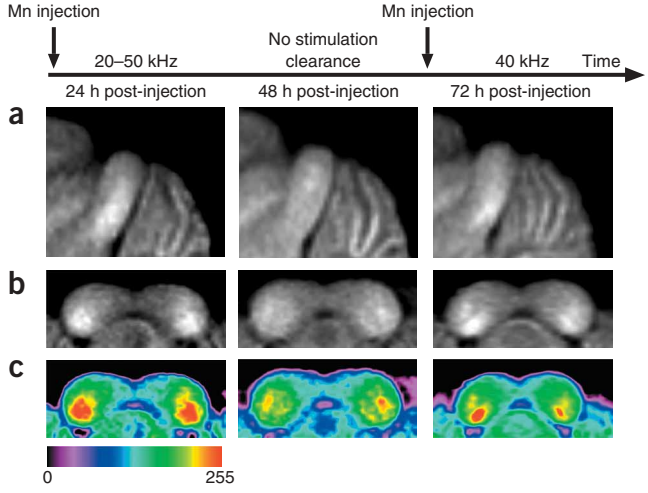

Figure 5 MEMRI can be used for longitudinal imaging studies. Averaged sagittal (**a**) and coronal (**b**) images of the IC after injection of $MnCl_2$ and 24 h of exposure to 20–50 kHz noise (left), after a subsequent 24 h with no defined stimulation (center), and after an additional injection of a half-dose of $MnCl_2$ and exposure to the 40 kHz pure tone for 24 h (right). (**c**) Coronal maps encoded in color to make the enhancement patterns easier to see (color scale shown below).

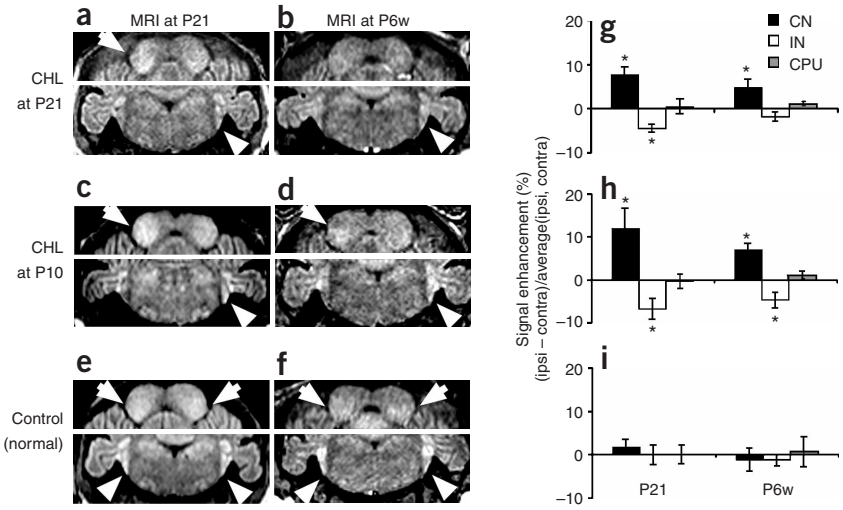

Figure 6 MEMRI demonstrates differences in sound-evoked activity in mice experiencing CHL at distinct developmental stages. (**a**–**d**) Mice with unilateral CHL at P21 (**a**,**b**) and P10 (**c**,**d**) and imaged at P21 (**a**,**c**) and P6w (**b**,**d**). (**e**,**f**) Comparisons to normal (control) mice, imaged at P21 (**e**) or P6w (**f**). Enhancement in CN (arrowheads, lower panels) and IC (arrows, upper panels) is marked. (**g**–**i**) Quantitative analysis of the ipsilateral-contralateral signal differences for CN, IC and (control) CPu in mice experiencing unilateral CHL at P21 ($n = 7$; **g**), and P10 ($n = 7$; **h**), and in normal mice ($n = 7$; **i**). Statistically significant MEMRI enhancement is marked with an asterisk (*).

were maintained for 24 h in their normal mouse room environment with no defined stimulation before a second MRI to assess short-term Mn^{2+} clearance from the IC. Each mouse was then injected a second time with $MnCl_2$ and exposed to 24 h of 40-kHz stimulation before the third and final MRI. There was an obvious shift from a broadband response to a 40 kHz pure-tone MEMRI enhancement pattern between the first and final MRI in each mouse, with partial clearance of the IC MEMRI signal at the intermediate time point ($n = 4$; **Fig. 5**). These results demonstrate that longitudinal MEMRI brain mapping studies can be performed in individual mice.

Developmental stage–dependent response to hearing loss

The second and third postnatal weeks represent a dynamic period in the development of auditory brain function in mice. During this time window, mice are susceptible to permanent alterations in auditory brain activity if reared under conditions of particular sustained sound stimulation[12,17]. In humans, early hearing loss can produce permanent changes in central anatomy and physiology[18,19]. Therefore, we sought to determine whether MEMRI could detect altered levels of activity associated with hearing loss at early developmental stages versus adult stages.

To examine developmental differences in MEMRI enhancement, we induced CHL at P10, before the onset of hearing, and at P21, when many neural properties have become adult-like in mice[20]. Similar to our initial experiments performed on mice experiencing unilateral CHL at 6 weeks (P6w), mice experiencing unilateral CHL at both early stages showed significant MEMRI enhancement in the ipsilateral CN and contralateral IC (**Fig. 6a–d**), with reference to the functional ear, whereas no difference was observed between the two sides of CN or IC in normal control mice (**Fig. 6e**,**f**). We performed statistical analysis (two-tailed *t*-test) comparing results in normal mice ($n = 7$) and mice experiencing unilateral CHL at either P10 ($n = 7$) or P21 ($n = 7$). Each mouse was injected with $MnCl_2$ and exposed to 24 h of broadband (1–59 kHz) stimulation before MRI acquisition at either P21 or P6w. At P21, there were significant ipsilateral-contralateral CN and IC signal differences in mice experiencing unilateral CHL at either P10 or P21 ($P < 0.0003$ compared with either CPu or normal CN/IC, **Fig. 6g–i**). Furthermore, there was a significant increase in the differential CN and IC signals measured in P10 unilateral CHL mice compared with P21 unilateral CHL mice ($P < 0.05$). In the same mice analyzed again at P6w, the P10 unilateral CHL mice showed significant differences in both CN ($P < 0.0003$, compared with CPu or normal CN) and IC ($P < 0.015$, compared with CPu or normal IC), whereas the P21 unilateral CHL mice showed a significant difference only in CN ($P < 0.001$), not in IC (**Fig. 6g–i**). Moreover, the age-dependent differences persisted into adulthood (P6w), with significantly greater differential CN and IC signal levels measured in P10 CHL mice than in P21 CHL mice ($P < 0.05$). These results indicate that conductive hearing loss at an early age leads to large and persistent changes in auditory brain function.

For longitudinal studies, it is important to determine the effect of an earlier injection of $MnCl_2$ on subsequent MEMRI measurements. In mice imaged twice, at P21 and then again at P6w, pre-injection T1-weighted images at P6w showed that Mn^{2+} enhancement from previous MEMRI experiments at P21 had cleared (**Supplementary Fig. 3**). These results are consistent with a recent report showing clearance of Mn^{2+} enhancement in the rat brain 14 d after intravenous injection of $MnCl_2$ (ref. 8). Notably, there were no differences in quantitative MEMRI data obtained at P6w, comparing unilateral CHL mice imaged at P21 and P6w with mice imaged once only at P6w (**Supplementary Fig. 3**), providing further support for the feasibility of longitudinal MEMRI studies. These results demonstrate the feasibility of using MEMRI to analyze neuroplasticity-related changes in sound-evoked activity during auditory brain development in the mouse.

DISCUSSION

MEMRI is an effective tool for auditory brain mapping

The results presented in this paper clearly demonstrate the utility of MEMRI for auditory brain mapping in mice after simple intraperitoneal injection of $MnCl_2$. The current protocol enables detection of accumulated activity in auditory brainstem nuclei after a long (24 h) exposure to repetitive sound stimulation in awake, normally behaving mice. Moreover, the MEMRI signal level within each auditory nucleus is highly consistent and provides a relative measure of sound-evoked activity with negligible contribution from MRI scanner noise (**Supplementary Note**). We have demonstrated the high spatial sensitivity of MEMRI in tonotopic maps of the mouse inferior colliculus. Furthermore, we have shown the feasibility of longitudinal imaging studies in individual mice and have demonstrated that changes in activity level associated with early hearing loss can be analyzed with MEMRI. In particular, our results show that early conductive hearing loss leads to a significant and persistent increase in auditory brainstem activity in mice.

Insights into the development of auditory brain function

In the auditory system, the exact nature of the neuroplasticity changes associated with deprivation of sound experience during development is not well understood (**Supplementary Note**). CHL in children, for example as a result of otitis media (middle ear infection), is known to induce deficits in binaural processing[21] and has been associated with delays in the acquisition of language and communication skills[22]. Animal models of CHL, used to study neuroplasticity changes associated with deprivation of auditory input during development, may therefore provide new insights and understanding of this increasingly prevalent childhood condition. Our results show that sound-evoked activity in the auditory midbrain of mice with unilateral CHL is predominantly contralateral to the functional ear, independent of the developmental stage at which hearing loss occurs. Furthermore, unilateral hearing loss at an early developmental stage (P10) biases the response towards the functional ear, compared with mice experiencing unilateral CHL at a later stage (P21). These results demonstrate the utility of MEMRI for analyzing altered patterns of activity associated with neuroplasticity changes in the developing mouse brain.

Comparison to previous MEMRI approaches

In previous studies, MEMRI has been used for *in vivo* axonal tract tracing in mice[23], primates[24] and birds[25] using stereotaxic injections of $MnCl_2$ into specific brain regions. Moreover, MEMRI tract tracing in songbirds was used to demonstrate activity-related differences in Mn^{2+} uptake in axonal projections induced by exposure to specific songs[25]. While these methods have the potential to show activity-related uptake and axonal transport of Mn^{2+}, the experimental procedure and results are different from our approach, in which Mn^{2+} is delivered into the brain systemically and accumulates specifically in the regions of neural activity induced by defined repetitive stimulation.

Previous implementations of MEMRI for activity imaging were limited to acute invasive studies in surgically cannulated rats[3–5] or were specific to the olfactory system[6]. The significance of the current studies is that intraperitoneal injection of $MnCl_2$ is easily implemented in mice, even at early postnatal stages[9], enabling mapping of sound-evoked activity in awake, normally behaving mice over a wide range of developmental stages. Furthermore, intraperitoneal injection is not specific for any particular brain region, so experiments analogous to those described in this paper can likely be designed and implemented in the future for other sensory systems in mice.

In our studies, significant MEMRI enhancement was detected in ascending auditory nuclei in the brainstem (CN, IC) and thalamus (medial geniculate nucleus), but not in the auditory cortex (**Fig. 2**). It is possible that the current protocol does not provide sufficient dose or length of time for the Mn^{2+} ions to diffuse to the auditory cortex, which is farther removed from the ventricular layers and therefore exposed to a lower level of Mn^{2+} than nuclei in the descending pathway. In addition, there may be a tract-tracing component to the Mn^{2+} enhancement, such that additional time is required for Mn^{2+} to be transported through projections from lower to higher auditory nuclei (**Supplementary Note**).

Our data are most consistent with the ventricular diffusion mechanism, as enhancement was highest in the CN and medial geniculate nucleus, which are immediately adjacent to ventricles, whereas enhancement was least in the auditory cortex, which is farthest removed from the ventricles, and intermediate in the IC, which is at an intermediate distance to the ventricles (**Fig. 2b**). In addition, we have performed preliminary experiments in which mice were injected with $MnCl_2$, maintained in a quiet environment for 16–20 h and imaged with MRI to verify that Mn^{2+} had cleared from the ventricles and blood, after which they were exposed to 40-kHz stimulation and imaged again. In those mice, we observed 40 kHz IC enhancement patterns similar to those obtained with the standard protocol ($n = 3$; data not shown), showing that accessibility to ventricular Mn^{2+} was not required for MEMRI activity detection. Furthermore, the nonspecific MEMRI enhancement at 16–20 h was similar in both CN and IC, showing that early Mn^{2+} uptake in the CN was not required to detect subsequent frequency-specific enhancement in the IC and suggesting that tract tracing is not the main source of sound-evoked enhancement in the ascending pathway.

In the auditory cortex, it is also possible that the more complex circuitry and/or habituation to repetitive stimulation precluded measurements of accumulated activity by MEMRI. At this point it is not clear why the cortex did not show Mn^{2+} accumulation in these studies. We conclude that the current MEMRI protocol is best suited for detecting activity in the brainstem and thalamus, in deep nuclei that can be examined by no other neuroimaging approach.

Comparison to alternative brain mapping methods

Previous studies to map activity in the mouse brain have largely used electrophysiology, which yields high resolution in defined nuclei but is difficult to perform and does not provide a method for functional mapping at the whole brain or sensory system level. Although optical imaging approaches enable measurements of intrinsic signals[26] and detection of activity-related fluorescent probes in genetically modified mice[27], these are invasive methods that can be used only in the superficial cortex after removing or thinning the skull. There are currently no established noninvasive *in vivo* neuroimaging approaches available for functional analysis of deeper brain regions in mice. In these first studies of the mouse central auditory system, our results are in excellent agreement with electrophysiological tonotopic maps in mice[13] and with previous measurements of neuronal metabolic activity, using *ex vivo* 2-deoxyglucose autoradiography in gerbils[10]. More generally, the MEMRI activity maps shown in this study have a number of similarities to 2-deoxyglucose maps[28], both providing the means to examine regions of accumulated neuronal activity in animals under normal conditions or after exposure to prolonged periods of a defined stimulation procedure. MEMRI has the obvious advantage that volumetric image data are acquired *in vivo*, enabling longitudinal imaging studies in individual animals. Although positron emission tomography (PET) enables *in vivo* imaging in humans, directly analogous to 2-deoxyglucose, unfortunately even with the best available micro-PET systems, effective brain mapping in mice is impossible due to the limited (1–2 mm) spatial resolution[29].

The MEMRI method described in this paper provides a unique noninvasive, whole-brain approach for mapping neural activity with high spatial resolution in mice. By combining MEMRI brain mapping with the rich resource of defined transgenic and mutant mouse strains, critical links can be made between genetics, neurodevelopment and adult brain function.

METHODS

Mouse surgery to induce CHL. The mice used in these studies were maintained under protocols approved by the Institutional Animal Care and Use Committee at New York University School of Medicine. Surgery was performed on Swiss Webster female mice to induce either bilateral or unilateral conductive hearing loss (CHL) at postnatal day 10 (P10), P21 and at postnatal week 6 (P6w). (For each mouse, the day of birth was denoted P0. For mice denoted 'P21,' surgery was performed between P20 and P21. MRI data at 'P21' was acquired starting 22–24 h after injection of $MnCl_2$, when the mice were between P21 and P22 days old. Mice denoted 'P6w' were staged between P40–44 days old.) Mice were anesthetized during surgery with isoflurane (5% isoflurane in air for 3 min to

induce anesthesia, and maintained with 1–1.5% isoflurane in air), delivered with an isoflurane vaporizer/anesthesia machine (VMS Matrix) using a custom nosecone. All surgeries were performed using a surgical microscope. At P21 and P6w, the tympanic membrane was punctured and the malleus removed, accessing the ear directly through the aural canal with fine forceps. At P10, a post-auricular incision was made to expose the external auditory canal and make a small opening through which the tympanic membrane was punctured and the malleus removed. In some P10 mice, a sham operation was performed, exposing the auditory canal and then closing the wound without further manipulation. The facial nerve was identified and avoided during the surgery, and the stapes was monitored to ensure its integrity and stability while removing the malleus. A small piece of compressed, sterile gelfoam was inserted into the middle ear cavity to suppress any minor bleeding. The small (2–3 mm) wound was closed with cyanoacrylate glue, and healed within 1–2 days. The entire surgical procedure took less than 5 min per ear. Following surgery, each mouse recovered for ~40 min on a warming pad (37 °C) and was returned to its cage after regaining full mobility. The mice showed no signs of distress or pain after these minimal surgeries. There was no obvious difference in auditory canal structures, comparing adult mice surgically manipulated at P10 or P21.

$MnCl_2$ administration. $MnCl_2$ was administered to mice in the form of an intraperitoneal (i.p.) injection. A 30 mM solution of $MnCl_2$ in isotonic saline (0.9% NaCl in water) was injected at a dose of 0.4 mmol/kg body weight. In practical terms, this translated into an easily performed i.p. injection of 0.2–0.4 ml $MnCl_2$ solution into 15- to 30-g mice (typical weights between P21 and P6w). A similar volume of saline was injected into control mice. In mice undergoing surgery at P21 or P6w, each mouse was allowed to recover for 1 h before being injected with $MnCl_2$. The $MnCl_2$ dose used in these studies was similar to the dose used in previous reports using MEMRI for structural imaging of the mouse brain[7–9], and provided clear T1-weighted MRI enhancement in a number of brain regions (**Fig. 1**). This dose was well below those used in previous studies of Mn-induced neurotoxicity[30]. We did not observe any abnormal behavior after i.p. injections of $MnCl_2$, up to 3 months later.

Acoustic stimulation experimental system. Sound stimulation in these studies consisted of signals covering frequency ranges audible to mice (1–59 kHz, 20–50 kHz and 40 kHz; **Supplementary Fig. 1**). The broadband (1–59 kHz, 20–50 kHz) signals were simultaneously frequency modulated (4 Hz) and amplitude modulated (5 Hz; peak level ≤95 dB sound peak level, SPL), whereas the 40 kHz pure-tone signal was amplitude modulated only. The acoustic waveforms were generated on a programmable HP8940A Multifunction Synthesizer (Hewlett Packard), amplified with a high fidelity T1005 audio amplifier (Epinions) and delivered through a Powerline 037 speaker (CTS). The speaker was mounted inside a Mac-1 acoustic isolation chamber (Industrial Acoustics) lined with polyurethane anechoic wedge panels (Acoustics First). Mice were allowed to behave normally, with unrestricted access to food and water, in standard mouse micro-isolator cages kept inside the acoustic chamber during the 24-h period of sound exposure or silence (control). The amplitude and spectral characteristics of the sound stimuli and background (room and MRI scanner) noises were measured with a multichannel spectrum analyzer (Bruel & Kjaer 3550) using a one-quarter–inch free-field condenser microphone and calibrated with a Model 4294 vibration reference source (**Supplementary Fig. 1**).

MRI data acquisition. MRI was performed on a micro-imaging system (MRRS) consisting of a 7-T horizontal magnet (Magnex Scientific) with actively shielded gradients (Magnex: 250-mT/m gradient strength; 200-μs rise time) and a custom 22-mm (inner diameter) Helmholtz mouse head coil or a 25-mm quadrature Litz mouse head coil (Doty Scientific). The coils were incorporated into a custom holder with a tooth bar to immobilize the head, and a nosecone for gas anesthesia (1–1.5% isoflurane in air), delivered with an isoflurane vaporizer/anesthesia machine (VMS Matrix). T1-weighted brain images were acquired with a 3D gradient echo pulse sequence (echo time, TE = 4 ms; repetition time, TR = 50 ms; flip angle = 65°), resulting in a volumetric image set covering the entire brain, with isotropic spatial resolution of 100 μm in a total imaging time of 1 h 50 min per mouse.

MRI data analysis. Volumetric MR image data were displayed and analyzed quantitatively with Analyze (v5.0, AnalyzeDirect). Through comparison of MR images with a mouse brain atlas (The Mouse Brain Library, http://www.mbl.org), we defined standard ROIs for quantitative analysis of MEMRI enhancement in auditory brain nuclei. ROIs were defined in multiple slices through each nucleus (**Fig. 2**). The signal intensity (SIN) mean and distribution (histogram) was measured in each ROI. In comparing MEMRI results from normal and bilateral CHL mice, differences may be interpreted equivalently as either signal enhancement in normal mice or signal loss in mice with CHL. Since MEMRI signal levels reflect MR contrast enhancement in brain regions with higher uptake of Mn^{2+}, our analyses were based on signal enhancement in normal mice compared with the (control) mice with CHL.

The caudate putamen (CPu) was used as an internal control for each mouse, as MEMRI enhancement in this region was independent of sound stimulation (**Fig. 3**). Therefore, the mean SINs in the auditory nuclei (CN, IC) were normalized to those in the CPu. For experiments involving unilateral hearing loss, analysis involved comparisons between SINs measured ipsilaterally and contralaterally to the functional ear:

$$(SIN_{ipsi} - SIN_{contra}) / \text{average}\,(SIN_{contra,}\ SIN_{ipsi}).$$

Three-dimensional images of the IC were generated with Amira (v3.1, Mercury Computer Systems-TGS) for the tonotopic mapping experiments. In each experimental group, the volumetric MRI data from each mouse brain were extracted, co-registered and averaged using the 3D image registration tools in Amira. The IC was then segmented from the averaged 3D brain images using an interactive threshold-based region-growing algorithm. Within each averaged 3D IC dataset, histograms were analyzed and enhanced regions were defined to contain all voxels with signal intensity greater than 15% above the average signal level in the CPu, the control brain region of each mouse. This criterion was selected based on the data showing an approximate 15% increase in active IC signal level compared with CPu (**Fig. 3f**). These enhanced voxels were then reassigned an arbitrary color (red) and were displayed in surface renderings representing the volumetric regions of activity (**Fig. 4e–h**). Measurements were made of IC volume and active (enhanced) volume (**Fig. 4i,j**) and position, defined as the distance between the centroid of the active volume and the centroid of the (complete) IC volume in each mouse (**Fig. 4k**). The depth of the 40-kHz centroid, below the dorsal surface of the IC, was measured and expressed as a percentage of the full dorsal-ventral extent of the IC, in both MEMRI and electrophysiological maps of the mouse IC[13].

In some cases, averaged images from Amira were imported into Photoshop (v7.0, Adobe), and the grayscale values reassigned using a color standard scale to facilitate detection of the active volumes (**Fig. 5**).

Statistical analysis. All data are presented as mean ± s.d. and were analyzed using two-tailed Student *t*-test or one-way ANOVA. Statistical significance was set at $P < 0.05$ and is indicated on figures with an asterisk (*). The specific test, *P*-value(s) and *F*-statistics (ANOVA) for each comparison are described in the Results section.

Note: Supplementary information is available on the Nature Neuroscience website.

ACKNOWLEDGMENTS

This research was supported by US National Institutes of Health grants NS38461 and DC06892 (D.H.T.). We thank A. Joyner and G. Fishell (Skirball Institute, NYU School of Medicine) for critical review of this paper. We also thank C. Moreno and D. Rubin for technical assistance in the initial stages of this project and J. Lefman for advice on the volumetric display and analysis routines used for tonotopic mapping. Finally, D.H.T. thanks R. Menon (Robarts Institute, University of Western Ontario) for originally drawing his attention to the potential of MEMRI for activity mapping.

COMPETING INTERESTS STATEMENT

The authors declare that they have no competing financial interests.

Received 24 January; accepted 9 May 2005
Published online at http://www.nature.com/natureneuroscience/

1. Ogawa, S., Lee, T.M., Kay, A.R. & Tank, D.W. Brain magnetic resonance imaging with contrast dependent on blood oxygenation. *Proc. Natl. Acad. Sci. USA* **87**, 9868–9872 (1990).
2. Narita, K., Kawasaki, F. & Kita, H. Mn and Mg influxes through Ca channels of motor nerve terminals are prevented by vermapil in frogs. *Brain Res.* **510**, 289–295 (1990).

3. Lin, Y. & Koretsky, A.P. Manganese ion enhanced T1-weighted MRI during brain activation: an approach to direct imaging of brain function. *Magn. Reson. Med.* **38**, 378–388 (1997).
4. Duong, T.Q., Silva, A.C., Lee, S.P. & Kim, S.G. Functional MRI of calcium-dependent synaptic activity: cross correlation with CBF and BOLD measurements. *Magn. Reson. Med.* **43**, 383–392 (2000).
5. Aoki, I., Naruse, S. & Tanaka, C. Manganese-enhanced magnetic resonance imaging (MEMRI) of brain activity and applications to early detection of brain ischemia. *NMR Biomed.* **17**, 569–580 (2004).
6. Pautler, R.G. & Koretsky, A.P. Tracing odor-induced activation in the olfactory bulbs of mice using manganese-enhanced magnetic resonance imaging. *Neuroimage* **16**, 441–448 (2002).
7. Watanabe, T., Natt, O., Boretius, S., Frahm, J. & Michaelis, T. *In vivo* 3D MRI staining of mouse brain after subcutaneous application of $MnCl_2$. *Magn. Reson. Med.* **48**, 852–859 (2002).
8. Aoki, I., Wu, Y.J., Silva, A.C., Lynch, R.M. & Koretsky, A.P. *In vivo* detection of neuroarchitecture in the rodent brain using manganese-enhanced MRI. *Neuroimage* **22**, 1046–1059 (2004).
9. Zaim Wadghiri, Y. *et al.* Manganese-enhanced magnetic resonance imaging (MEMRI) of mouse brain development. *NMR Biomed.* **17**, 613–619 (2004).
10. Tucci, D.L., Cant, N.B. & Durham, D. Conductive hearing loss results in a decrease in central auditory system activity in the young gerbil. *Laryngoscope* **109**, 1359–1371 (1999).
11. Ryugo, D.K., Willard, F.H. & Fekete, D.M. Differential afferent projections to the inferior colliculus from the cochlear nucleus in the albino mouse. *Brain Res.* **210**, 342–349 (1981).
12. Sanes, D.H. & Constantine-Paton, M. The sharpening of frequency tuning curves requires patterned activity during development in the mouse. *Mus musculus. J. Neurosci.* **5**, 1152–1166 (1985).
13. Romand, R. & Ehret, G. Development of tonotopy in the inferior colliculus. I. Electrophysiological mapping in house mice. *Brain Res. Dev. Brain Res.* **54**, 221–234 (1990).
14. Sterbing, S.J. & Schrott-Fischer, A. Neuronal responses in the inferior colliculus of mutant mice (Bronx waltzer) with hereditary inner hair cell loss. *Hear. Res.* **177**, 91–99 (2003).
15. Ehret, G. Development of absolute auditory thresholds in the house mouse (*Mus musculus*). *J. Am. Audiol. Soc.* **1**, 179–184 (1976).
16. Willott, J.F. & Urban, G.P. Response properties of neurons in nuclei of the mouse inferior colliculus. *J. Comp. Physiol.* **127**, 175–184 (1978).
17. Webster, D.B. & Webster, M. Neonatal sound deprivation affects brain stem auditory nuclei. *Arch. Otolaryngol.* **103**, 392–396 (1977).
18. Sharma, A., Dorman, M.F. & Spahr, A.J. A sensitive period for the development of the central auditory system in children with cochlear implants: implications for age of implantation. *Ear Hear.* **23**, 532–539 (2002).
19. Emmorey, K., Allen, J.S., Bruss, J., Schenker, N. & Damasio, H. A morphometric analysis of auditory brain regions in congenitally deaf adults. *Proc. Natl. Acad. Sci. USA* **100**, 10049–10054 (2003).
20. Shnerson, A. & Pujol, R. Development: anatomy, electrophysiology, and behavior. In *The Auditory Psychobiology of the Mouse* (ed. Willot, J.F.) 395–425 (Charles C. Thomas, Springfield, Illinois, 1983).
21. Hall, J.W., Jr., Grose, J.H. & Pillsbury, H.C. Long-term effects of chronic otitis media on binaural hearing in children. *Arch. Otolaryngol. Head Neck Surg.* **121**, 847–852 (1995).
22. Schilder, A.G. *et al.* Long-term effects of otitis media with effusion on language, reading and spelling. *Clin. Otolaryngol.* **18**, 234–241 (1993).
23. Pautler, R.G., Silva, A.C. & Koretsky, A.P. *In vivo* neuronal tract tracing using manganese-enhanced magnetic resonance imaging. *Magn. Reson. Med.* **40**, 740–748 (1998).
24. Saleem, K.S. *et al.* Magnetic resonance imaging of neuronal connections in the macaque monkey. *Neuron* **34**, 685–700 (2002).
25. Tindemans, I., Verhoye, M., Balthazart, J. & Van Der Linden, A. *In vivo* dynamic ME-MRI reveals differential functional responses of RA- and area X-projecting neurons in the HVC of canaries exposed to conspecific song. *Eur. J. Neurosci.* **18**, 3352–3360 (2003).
26. Kalatsky, V.A. & Stryker, M.P. New paradigm for optical imaging: temporally encoded maps of intrinsic signal. *Neuron* **38**, 529–545 (2003).
27. Bozza, T., McGann, J.P., Mombaerts, P. & Wachowiak, M. *In vivo* imaging of neuronal activity by targeted expression of a genetically encoded probe in the mouse. *Neuron* **42**, 9–21 (2004).
28. Kennedy, C. *et al.* Mapping of functional neural pathways by autoradiographic survey of local metabolic rate with (^{14}C)deoxyglucose. *Science* **187**, 850–853 (1975).
29. Tai, Y.C. *et al.* MicroPET II: design, development and initial performance of an improved microPET scanner for small-animal imaging. *Phys. Med. Biol.* **48**, 1519–1537 (2003).
30. Shukakidze, A., Lazriev, I. & Mitagvariya, N. Behavioral impairments in acute and chronic manganese poisoning in white rats. *Neurosci. Behav. Physiol.* **33**, 263–267 (2003).